

# Flexible and Transparent Electrothermal Film Heaters Based on Graphene Materials

Dong Sui, Yi Huang,\* Lu Huang, Jiajie Liang, Yanfeng Ma, and Yongsheng Chen

**H**igh-performance and novel graphene-based electrothermal films are fabricated through a simple yet versatile solution process. Their electrothermal performances are studied in terms of applied voltage, heating rate, and input power density. The electrothermal films annealed at high temperature show high transmittance and display good heating performance. For example, the graphene-based film annealed at 800 °C, which shows transmittance of over 80% at 550 nm, can reach a saturated temperature of up to 42 °C when 60 V is applied for 2 min. Graphene-based films annealed at 900 and 1000 °C can exhibit high steady-state temperatures of 150 and 206 °C under an applied voltage of 60 V with a maximum heating rate of over 7 °C s<sup>-1</sup>. For flexible heating films patterned on polyimide, a steady-state temperature of 72 °C could be reached in less than 10 s with a maximum heating rate exceeding 16 °C s<sup>-1</sup> at 60 V. These excellent results, combined with the high chemical stability and mechanical flexibility of graphene, indicate that graphene-based electrothermal elements hold great promise for many practical applications, such as defrosting and antifogging devices.

## 1. Introduction

Two-dimensional electrothermal heating elements (films), especially transparent and flexible film heaters, have attracted growing interest for a wide range of applications including outdoor displays, vehicle window defrosters, heating retaining windows, and other heating systems.<sup>[1]</sup> The commercial film-like heater made from strips of a Fe–Cr–Al-based alloy has many disadvantages, such as its complicated fabrication process, opacity, heavy weight, rigidity, and low heating efficiency.<sup>[1c]</sup> Thus, indium tin oxide (ITO) has been widely used to prepare transparent heating films as it is optically transparent to visible wavelengths and has high electrical conductivity.<sup>[2]</sup> However, ITO has some drawbacks too, such as the limited availability of indium, intolerance

to acid or base, and fragility under mechanical bending deformation.<sup>[1b,3]</sup> Alternatives have been investigated to replace ITO. Ga-doped zinc oxide films that possess reasonable conductivity and transparency have also been investigated as transparent heaters because of their lower material cost and relatively lower deposition temperature compared to that of ITO.<sup>[1a,4]</sup> Carbon nanotubes (CNTs) possess excellent thermal,<sup>[5]</sup> electrical, and optical properties,<sup>[6]</sup> which are key factors that influence the performance of electrothermal films. Han and co-workers first fabricated transparent heating films using single-wall carbon nanotubes and an excellent heating performance was observed.<sup>[6]</sup> Since then, CNT film heaters have been investigated extensively and are proving to be an excellent potential heating element.<sup>[1b,1c,7]</sup>

Graphene, a 2D, atomically thick crystal material that consists of sp<sup>2</sup>-hybridized carbons, has attracted much attention all around the world since it was first isolated in 2004.<sup>[8]</sup> The amazing electronic properties of graphene result from its linear electron-dispersion relation,<sup>[9]</sup> room temperature quantum effects,<sup>[10]</sup> and ambipolar electric-field effects.<sup>[8]</sup> Moreover, its 2D aromatic conjugate structure also endows graphene with excellent mechanical,<sup>[11]</sup> optical,<sup>[12]</sup> and thermal conductive ( $\approx 5000 \text{ W m}^{-1} \text{ K}^{-1}$ ) properties.<sup>[13]</sup> These outstanding and unique properties have made graphene-based materials promising for many applications,<sup>[14]</sup> including

D. Sui, Prof. Y. Huang, L. Huang, Dr. J. J. Liang, Prof. Y. F. Ma, Prof. Y. S. Chen

Key Laboratory of Functional Polymer Materials and Center for Nanoscale Science and Technology  
Institute of Polymer Chemistry  
College of Chemistry Nankai University  
Tianjin, 300071, China  
E-mail: yihuang@nankai.edu.cn

DOI: 10.1002/smll.201101305

transparent electrodes,<sup>[3,15]</sup> field-effect transistors,<sup>[16]</sup> sensors,<sup>[17]</sup> drug-delivery systems,<sup>[18]</sup> polymer photovoltaics,<sup>[19]</sup> energy and gas storage,<sup>[20]</sup> nanocomposites,<sup>[21]</sup> and integrated circuits.<sup>[22]</sup> To date, various methods, such as mechanical exfoliation,<sup>[8]</sup> epitaxial growth,<sup>[23]</sup> chemical vapor deposition,<sup>[24]</sup> and exfoliation and reduction of graphene oxide (GO),<sup>[15]</sup> have been applied to prepare graphene sheets. Compared to other methods, chemical exfoliation allows for low cost, large-scale production, and imparts graphene with good solution processability and versatile chemical properties, which make it an excellent and practical choice for solution-processed flexible electronic applications. Thin graphene films with excellent mechanical flexibility and chemical stability can be easily prepared by spin-coating a GO solution onto various substrates, followed by chemical and/or high-temperature annealing and reduction.

With an easier processing procedure compared with that of CNTs, which can't be processed in solution without stabilization by a surfactant, graphene's super electrical and thermal conductivity, excellent optical transparency, and flexibility are expected to make it a superior choice of material for electrothermal applications. Unfortunately, to the best of our knowledge, there is still no such report about graphene for electrothermal heating applications. In this work, graphene electrothermal heating films/elements were fabricated on both quartz and flexible polyimide (PI) substrates utilizing a simple solution process beginning from GO followed by thermal annealing. It is demonstrated that these heating films/elements have a high performance, with films annealed at 800 °C (RGO-800) showing over 80% transmittance at 550 nm and reaching a steady-state temperature as high as 42 °C at an applied voltage of 60 V. Furthermore, the films annealed at higher temperatures of 900 and 1000 °C (RGO-900 and RGO-1000) have steady-state temperatures of 150 and 206 °C at 60 V, respectively, with a maximum heating rate of over 7 °C s<sup>-1</sup>. Flexible films with different thickness were formed on PI that exhibit good heating performances and fast response times. Specifically, a saturated temperature of over 70 °C can be reached within 10 s with a maximum heating rate over 16 °C s<sup>-1</sup> at 60 V. Importantly, these films are quite physically robust wherein repeated bending has only a slight influence on the film's thermal performance and sheet resistance.

## 2. Results and Discussion

### 2.1. Graphene Film Preparation and Characterization

Graphene oxide (GO) prepared through a modified Hummers method,<sup>[15]</sup> is a versatile precursor because the many oxygen-containing functional groups distributed on its basal plane and edges

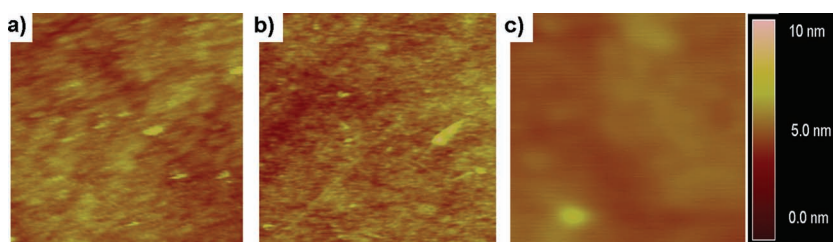


**Figure 1.** Typical tapping-mode AFM height images (2.5 μm × 2.5 μm) of graphene films on quartz: a) RGO-800, b) RGO-900, and c) RGO-1000, with surface roughnesses of 1.275, 0.859, and 0.556 nm, respectively.

enlarge interlamellar spacing and enable it to disperse in water.<sup>[25]</sup> In this work a GO aqueous solution with concentrations up to 10 mg ml<sup>-1</sup> were obtained by simple ultrasonication. While various methods have been developed to prepare graphene films, such as spray-coating,<sup>[26]</sup> spin-coating,<sup>[15]</sup> dip-coating<sup>[3]</sup> and vacuum filtration,<sup>[27]</sup> spin-coating was used in this study because this method can be manipulated facily and can afford more uniform films. Conductive graphene films were obtained by exposure of raw GO films to hydrogen iodide (HI) vapor followed by thermal treatment.<sup>[28]</sup>

The surface morphology of the fabricated graphene films deposited on quartz were first characterized by atomic force microscopy (AFM). Typical AFM height images are shown in **Figure 1**. All films display a continuous and homogeneous surface, which is attributed to the well-dispersed GO in the precursor solution and the simple spin-coating deposition method.

GO, whose conjugated aromatic structure is highly damaged in its preparation process, is actually an insulator. A chemical reduction in combination with thermal annealing needs to be used to recover its conducting network. It is well known that both sheet resistance and transmittance are largely influenced by reduction methods and annealing temperatures.<sup>[15]</sup> As presented in **Figure 2a**, a linear relationship between the voltage and current was observed for these graphene films, indicating good semiconducting behavior. As shown in **Table 1**, the sheet resistance determined by the *I*-*V* measurement could be greatly reduced from 6.079 kΩ □<sup>-1</sup> for RGO-800 to 1.568 kΩ □<sup>-1</sup> for RGO-900 and to 0.641 kΩ □<sup>-1</sup> for RGO-1000. Next, the optical transmittance of the films was evaluated and it as found that these films have a pretty flat and wide transmittance over the whole visible region, independent of the annealing temperature (Figure 2b).

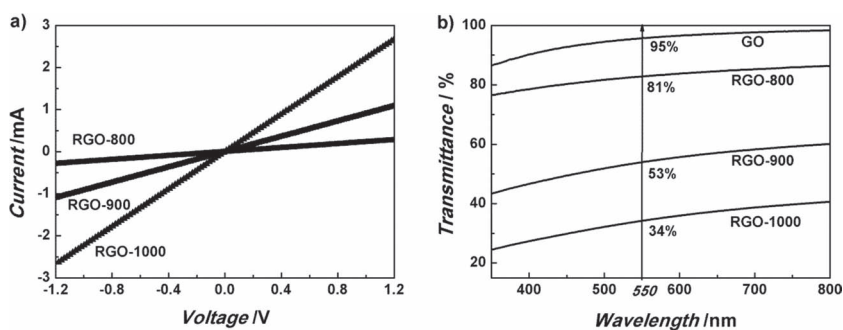


**Figure 2.** a) *I*-*V* measurement and b) optical transmittance spectra in the visible region of GO and reduced GO films deposited on quartz.

**Table 1.** Sheet resistance, conductivity, and thickness of different samples on quartz annealed at different temperatures.

Sample	Sheet resistance [k $\Omega$ square <sup>-1</sup> ]	Film conductivity [S cm <sup>-1</sup> ]	Film thickness [nm]
RGO-800	6.079	44.5	37
RGO-900	1.568	187.6	34
RGO-1000	0.641	445.7	35

Specifically,  $\approx 35$  nm-thick graphene films reduced under the annealing temperatures of 800, 900, and 1000 °C have transmittances of 81%, 53%, and 34%, respectively, at a wavelength of 550 nm. The trend of decreasing transmittance with increased annealing temperature has been observed in previous works, and has been attributed to the restoration of the  $\pi$ -electron system in the graphene structure.<sup>[15]</sup>

### 2.2. Electrothermal Performances of Films on Quartz

Direct current power was applied to the graphene films (valid heating area:  $2 \times 1.4$  cm<sup>2</sup>) deposited on quartz and their electrothermal performances investigated under ambient conditions, as demonstrated in **Figure 3**. After electrical power is supplied to the films, the surface temperature monotonically increases over time until a steady-state temperature is reached. For a given film, the steady-state temperature increases with increasing applied voltage. The higher the annealing temperature of the sample, the higher the steady-state temperature at a given applied voltage

(Figure 3d). Compared with the other two films, RGO-800, which has a relatively higher sheet resistance, displays the lowest steady-state temperature and the lowest heating rate at the same applied voltage. This may be attributed to the lower transduction of electrical energy into Joule-heating, based on the equation  $P = U^2/R$  (where  $P$  is power,  $U$  is the applied voltage, and  $R$  is the resistance). RGO-800 shows a steady-state temperature of 42 °C with a maximum heating rate of  $0.7$  °C s<sup>-1</sup> at a driving voltage of 60 V (see Figure 3a and the Supporting Information (SI), Figure S1), which is comparable to heating films prepared with single-walled carbon nanotubes (SWCNTs).<sup>[1b]</sup> Therefore, RGO-800 can be used as a transparent heating film considering its low electricity consumption (e.g., maximum input power density of less than  $0.175$  W cm<sup>-2</sup> (see SI, Figure S1)), and good transparency of higher than 75% over the whole visible region. Furthermore, as shown in Figure 3b,c, a higher heating rate and higher steady-state temperatures are observed for RGO-900 and RGO-1000, which benefit from lower sheet resistance. Both of these two samples can reach their steady-state temperatures in less than 2 min. A saturation temperature of 55 °C can be reached for RGO-900 when a voltage of 30 V is applied, which can be increased to 150 °C by increasing the voltage to 60 V. With regard to RGO-1000, the steady-state temperature at 60 V is up to 206 °C. Both of the two films show maximum heating rates of over  $7$  °C s<sup>-1</sup> at an applied voltage of 60 V (see SI, Figure S1), which is much higher than that of SWCNTs at the same voltage.<sup>[1b]</sup> Compared to the RGO-800, the RGO-900 and RGO-1000 samples can achieve a higher input power at the same applied voltage because of the improved conductivity resulting from the

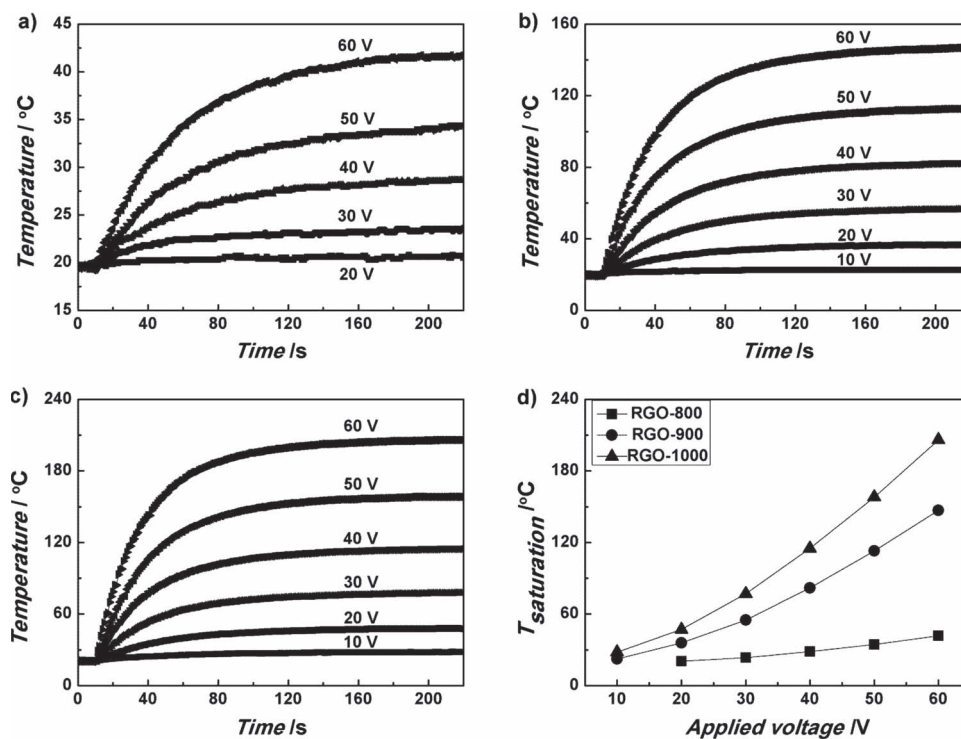


**Figure 3.** Electrothermal performance of graphene films ( $2 \text{ cm} \times 1.4 \text{ cm}$ ) deposited on quartz. Time versus temperature profiles with respect to different applied voltages for a) RGO-800, b) RGO-900, and c) RGO-1000. d) Steady-state temperatures versus the applied voltages.

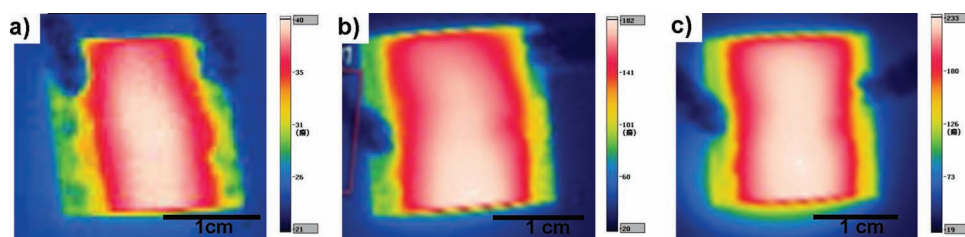


**Figure 4.** The infrared thermal images of a) RGP-800, b) RGO-900, and c) RGO-1000 at 60 V.

higher temperature of reduction. But the maximum input power density is still less than  $2 \text{ W cm}^{-2}$  (see SI, Figure S1).

**Figure 4** depicts the infrared thermal images of the graphene films at their steady-state temperatures under an applied voltage of 60 V. It should be noted that the temperature distribution of the graphene films at the applied voltages is rather homogeneous. This even distribution of heat may be attributed to the excellent thermal and electrical conductivity of graphene as well as the highly uniform surface of the graphene films. It should also be noted that the size of the films fabricated using the solution-based process outlined here is not limited to small sizes. Thus, it is possible to produce films for applications that require larger active areas.

With the excellent optical and electrothermal properties of these graphene films in hand, several immediate applications can be proposed. RGO-800, which possesses an improved light transmission over the other samples, could serve as a transparent film heater on either car or building windows. As a demonstration, frost of about 1 mm thickness was allowed to form on the back of the graphene film at  $-10^\circ\text{C}$  in a refrigerator and a defrosting test was carried out under the same conditions (see **Figure 5a,b**). As it is shown in **Figure 5c**, the frost on the surface of the heating element was completely removed after a voltage of 60 V was applied for only 2 min. Considering the excellent chemical stability, light weight, and high transparency of graphene, a graphene-based defroster is feasible for outdoor displays, the back and side windows of vehicles, and other equipment needing transparent heating films for either defrosting or temperature maintenance.

Though RGO-900 and RGO-1000 show improved electrothermal performance, it came at the cost of reduced transparency. Nevertheless, these films may find use in many other devices that need heating films but do not have the requirement of a high transmittance. For example, people are always bothered by the invisibility of rearview mirrors in vehicles and bathroom mirrors in winter because water vapor is always condensed on their surfaces. As such, the applications for these films could include antifogging for such mirrors. Here, a moisture removal device is fabricated by pasting RGO-900 on the back of a mirror and tested its antifog effect under the same conditions as mentioned above. As shown in **Figure 6a,b**, the image in the mirror

becomes totally indistinct after a thin layer of water was condensed on it. However, after applying a voltage of 60 V for 30 s to the heating film, the moisture on the mirror surface was removed and the visibility of the image was clearly recovered (**Figure 6c**). The excellent heating performances of these films also endows them with applications that need a high heating rate and a high steady-state temperature.

### 2.3. Flexible Heating Units on PI

Flexible heating films with different thickness on PI (valid heating area:  $2 \times 1.6 \text{ cm}^2$ ) were fabricated by simply spin-coating a solution of GO on PI followed by pre-reduction with HI vapor and thermal annealing at  $450^\circ\text{C}$ . Their electrothermal performances under different test conditions were studied. The mechanical robustness and flexibility of the films were investigated by repeatedly bending them 100 times (see inset of **Figure 7c**). It's important to note that after 100 bending cycles there is no visible change in the morphology and only a slight change in the resistance of these graphene films on PI substrates (both samples PI-1 and PI-2 with different thicknesses) was observed (see SI, Table S1). This outstanding performance may be attributed to the robustness and flexibility of the graphene films.

As shown in **Figure 7** and **Figure 8**, similar results are observed for the films on PI as for those on quartz substrates. The surface temperature of the film, when charged with electrical power, exhibits a fast monotonic rise until a saturation

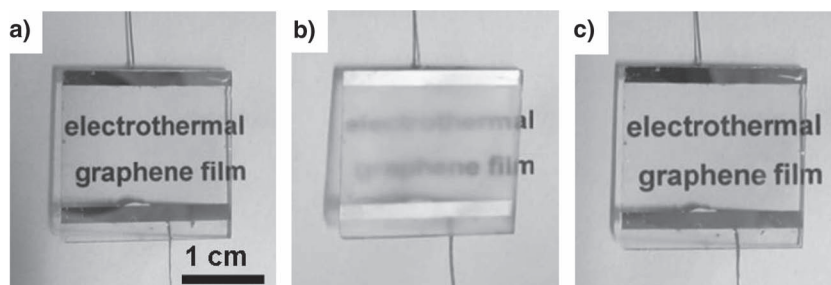


**Figure 5.** Frost removal performance results of RGO-800 before (a) and after (b) frost formed on the back of the film, and c) after heating at 60 V for 2 min.

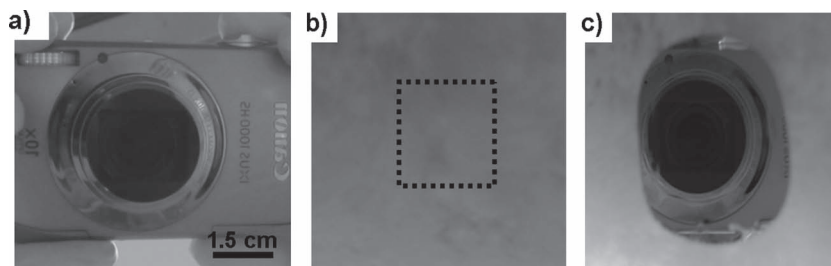


**Figure 6.** Moisture removal results of RGO-900, before (a) and after (b) water vapor condensed on the mirror surface, and c) after heating at 60 V for 30 s.

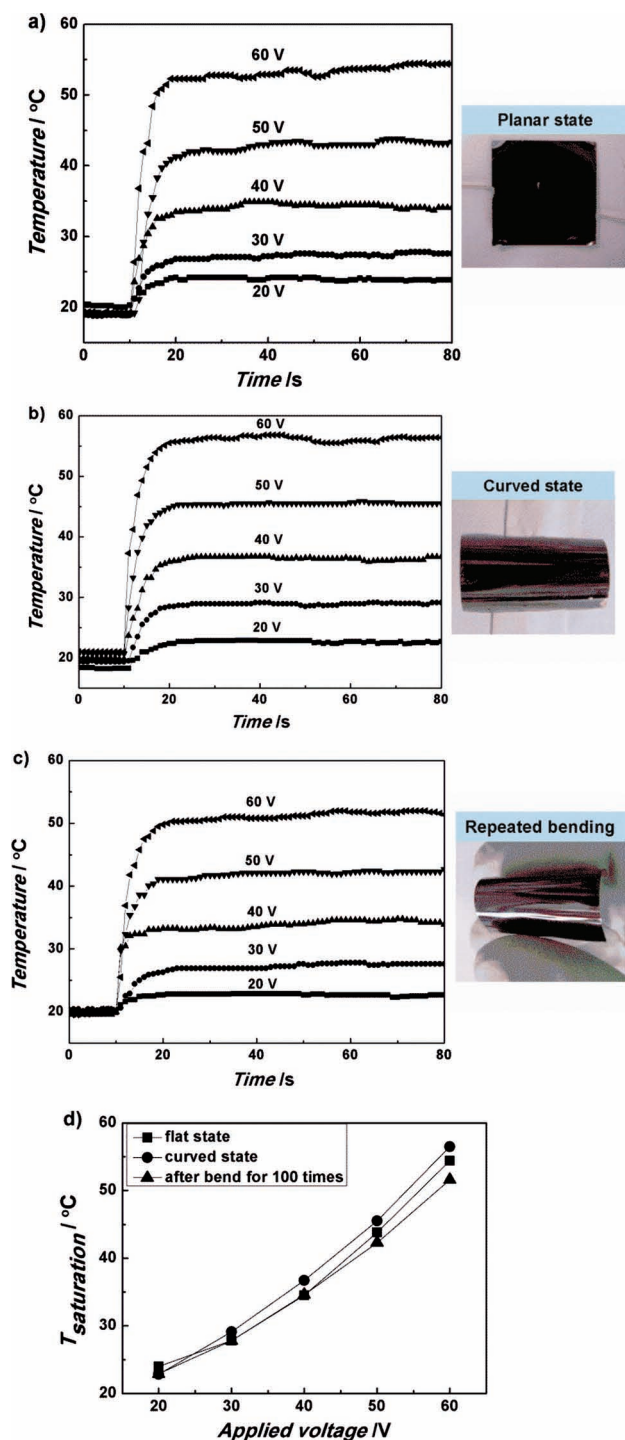


Figure 7. Time versus temperature profiles of PI-1 (2 cm × 1.6 cm) with respect to different applied voltages in a) planar and b) curved states, and c) after bending 100 times. d) Steady-state temperature versus applied voltage.

temperature is reached. The steady-state temperature of PI-1, which has a thickness of 45 nm, is over 50 °C at an applied voltage of 60 V, with the maximum heating rate exceeding 10 °C s<sup>-1</sup> (see SI, Figure S2), while the saturation temperature of PI-2, which has a thickness of 70 nm, is as high as 72 °C with heating rate of 16 °C s<sup>-1</sup> at 60 V (see SI, Figure S3). It

is obvious that the higher steady-state temperature of PI-2 is due to its lower sheet resistance. Moreover, compared to PI-1, a much smaller change in resistance for PI-2 was observed after repeatedly bending 100 times (see SI, Table S1), which may be attributed to the thicker film of PI-2. More importantly, repeated bending tests (over 100 times) of these flexible heating units has rather little impact on their electrothermal performance, as shown in Figure 7d and Figure 8c. The difference in steady-state temperature before and after 100 bending cycles is only about 2 °C, which may partially arise from convective heat transfer by the air flow adjacent to the film.

Furthermore, compared with the graphene films on quartz and glass substrates, these flexible graphene thermal heaters display even better electrothermal performance. The steady-state temperature of the graphene films on flexible PI was achieved within 10 s compared with ≈80 s using quartz, and the maximum heating rate at 60 V could exceed 16 °C s<sup>-1</sup> compared with 9 °C s<sup>-1</sup> using quartz (see SI, Figure S1,S3). Both the PI-1 and PI-2 samples under all testing conditions have a maximum input power density lower than 250 mW cm<sup>-2</sup> (see SI, Figure S2,S3). The better heating performance is due to the smaller thickness and smaller heat capacity of PI compared with quartz. Also, the temperature on the entire surface, regardless of whether the surface was in a planar or curved state, is rather even as the IR thermal images show (see SI, Figure S4). Consequently, not only is the electrothermal performance of these two heating units excellent, but also the heating rate and steady-state temperature could be adjusted by simply changing either the film thickness or the applied voltage. The electrothermal films fabricated here, with the advantages of flexibility, low energy consumption, and very fast heating times, could be used as heating units where both flexibility and high heating performance are required.

### 3. Conclusion

Graphene-based electrothermal heating elements with excellent heating performance and flexibility were fabricated through spin-coating a GO solution on quartz or PI and their electrothermal performances were studied in terms of heating rate and applied voltage. Heating films deposited on quartz show high transparencies and good heating effects. Devices for defrosting or antifogging based on these heating units were prepared and remarkable efficiencies were observed. Flexible graphene films formed on PI show exciting electrothermal and mechanical properties including fast heating rates and pretty robust endurance against repeated bending. We attribute these properties to the excellent electrical, thermal, optical, and mechanical properties of graphene. As a consequence of their chemical stability, mechanical flexibility, high transparency, light weight, and scalable production through easy solution processing, graphene films are excellent potential candidates for film heaters. Some notable applications include thermal control components for aircrafts, in medical equipment, or in home appliances as well as in many other industrial fields.

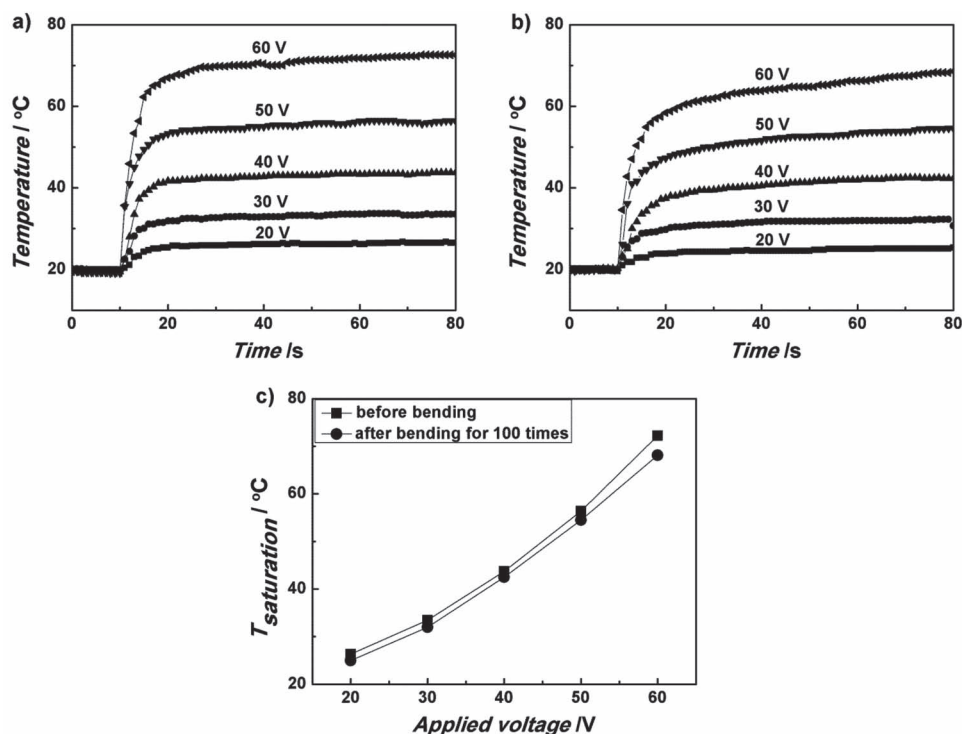


**Figure 8.** Time versus temperature profiles for PI-2 (2 cm  $\times$  1.6 cm) with respect to different applied voltages before (a) and after (b) bending 100 times. c) Steady-state temperature versus applied voltage.

## 4. Experimental Section

**Preparation of Graphene Oxide:** The starting material GO was prepared through a modified Hummers method reported elsewhere.<sup>[15]</sup> In brief, flake graphite (Qingdao Tianhe Graphite Co. Ltd., Qingdao, China, 20  $\mu\text{m}$ ) was oxidized by  $\text{NaNO}_3$  and  $\text{KMnO}_4$  in concentrated  $\text{H}_2\text{SO}_4$  and reacted with 30%  $\text{H}_2\text{O}_2$  to complete oxidation, then washed thoroughly with dilute  $\text{H}_2\text{SO}_4$ , dilute HCl, and deionized water. Lastly the GO was isolated by centrifugation and dried to obtain a brown solid that can be dispersed in water to a concentration of up to 15  $\text{mg mL}^{-1}$  by simple ultrasonication.

**Deposition and Reduction of Graphene Oxide Films:** Graphene oxide was dispersed in water at a concentration of 10  $\text{mg mL}^{-1}$  by ultrasonication for 2 h. The GO solution was deposited on hydrophilic substrates with dimensions of 2.0 cm  $\times$  2.0 cm (such as quartz, glass, and PI) by spin coating method. Generally speaking, for the films on quartz and glass (2 cm  $\times$  2 cm  $\times$  1 mm), the GO solution coated on substrates was allowed to stand for 30 s to wet the surface, after which the substrates was spin at 500 rpm for 9 s and 3000 rpm for 30 s. Then the films were dried at room temperature for 5 h and then at 80 °C for 5 h. After that, the GO films were placed on filter papers saturated with an HI solution and sealed in a container which was put in a constant-temperature oven at 100 °C for 10 h, wherein pre-reduction was accomplished from exposure to HI vapor. The films were further reduced by thermal annealing at the rate of 5 °C  $\text{min}^{-1}$  and held at their target temperatures for 3 h under the atmosphere of Ar/ $\text{H}_2$  (9:1 vol.) in a quartz tube furnace, then cooled to room temperature naturally.

Different annealing temperatures were carried out to evaluate the transparency and electrothermal performance. Three heating films, RGO-800, RGO-900, and RGO-1000, were made, representing the samples annealed at 800, 900, and 1000 °C, respectively. Films deposited on PI (2 cm  $\times$  2 cm  $\times$  50  $\mu\text{m}$ ) with different thickness were prepared using a similar method. After pre-reduction with HI vapor the films were heated to 450 °C at a rate of 5 °C  $\text{min}^{-1}$ , held at 450 °C for 5 h under the same atmosphere mentioned above, and then cooled to room temperature naturally.

**Characterization:** After reduction/annealing treatment, gold electrodes with a width of 2 mm and thickness of 50 nm were deposited onto the films through a shadow mask and their sheet resistances were measured with a semiconductor parametric analyzer (Keithley 4200, Keithley Instruments Inc.). Transmittance in the visible region was measured using UV-vis-NIR spectrophotometer (JASCO V-570). Tapping-mode atomic force microscopy (AFM) measurements were performed using a Multimode SPM from Digital Instruments with a Nanoscope IIIa Controller to characterize the surface morphology of the graphene films. The thickness of graphene film was measured by a profilometer (XP-2 AMBIO Technology). For films deposited on PI, silver paste electrodes were used instead of gold and the sheet resistance was determined with a digital multimeter (UT61B). The voltage was supplied by a DC power source (Zhaoxin RXN-6050) and a digital multimeter was used to measure the current. The average surface temperature of the films was measured in real time by an infrared thermometer (MASTECH MS6550A). The surface temperature distribution was characterized by an infrared thermal imager (Raytek RAYPI20).

## Supporting Information

Supporting Information is available from the Wiley Online Library or from the author.

## Acknowledgements

The authors gratefully acknowledge financial support from the NSFC (Grants 50933003, 50902073 and 50903044), MOST (Grants 2011CB932602 and 2011DFB50300), and Tianjin City (Grant 10ZCGHHZ00600).

- [1] a) J. H. Kim, B. Du Ahn, C. H. Kim, K. A. Jeon, H. S. Kang, S. Y. Lee, *Thin Solid Films* **2008**, *516*, 1330–1333; b) T. J. Kang, T. Kim, S. M. Seo, Y. J. Park, Y. H. Kim, *Carbon* **2011**, *49*, 1087–1093; c) W. Zi Ping, W. Jian Nong, *Physica E* **2009**, *77*–81.
- [2] a) J. Ederth, P. Johnsson, G. A. Niklasson, A. Hoel, A. Hultaker, P. Heszler, C. G. Granqvist, A. R. van Doorn, M. J. Jongerius, D. Burgard, *Phys. Rev. B* **2003**, *68*, 155410–155419; b) K. Im, K. Cho, J. Kim, S. Kim, *Thin Solid Films* **2010**, *518*, 3960–3963.
- [3] X. Wang, L. J. Zhi, K. Mullen, *Nano Lett.* **2008**, *8*, 323–327.
- [4] B. D. Ahn, S. H. Oh, D. U. Hong, D. H. Shin, A. Moujoud, H. J. Kim, *J. Cryst. Growth* **2008**, *310*, 3303–3307.
- [5] E. Pop, D. Mann, Q. Wang, K. Goodson, H. J. Dai, *Nano Lett.* **2006**, *6*, 96–100.
- [6] Y. H. Yoon, J. W. Song, D. Kim, J. Kim, J. K. Park, S. K. Oh, C. S. Han, *Adv. Mater.* **2007**, *19*, 4284–4287.
- [7] a) D. Kim, H. C. Lee, J. Y. Woo, C. S. Han, *J. Phys. Chem. C* **2010**, *114*, 5817–5821; b) H. S. Jang, S. K. Jeon, S. H. Nahm, *Carbon* **2011**, *49*, 111–116.
- [8] K. S. Novoselov, A. K. Geim, S. V. Morozov, D. Jiang, Y. Zhang, S. V. Dubonos, I. V. Grigorieva, A. A. Firsov, *Science* **2004**, *306*, 666–669.
- [9] M. I. Katsnelson, *Mater. Today* **2007**, *10*, 20–27.
- [10] Y. B. Zhang, Y. W. Tan, H. L. Stormer, P. Kim, *Nature* **2005**, *438*, 201–204.
- [11] C. Lee, X. D. Wei, J. W. Kysar, J. Hone, *Science* **2008**, *321*, 385–388.
- [12] R. R. Nair, P. Blake, A. N. Grigorenko, K. S. Novoselov, T. J. Booth, T. Stauber, N. M. R. Peres, A. K. Geim, *Science* **2008**, *320*, 1308–1308.
- [13] a) A. A. Balandin, S. Ghosh, W. Z. Bao, I. Calizo, D. Teweldebrhan, F. Miao, C. N. Lau, *Nano Lett.* **2008**, *8*, 902–907; b) D. L. Nika, S. Ghosh, E. P. Pokatilov, A. A. Balandin, *Appl. Phys. Lett.* **2009**, *94*, 203103–203105; c) D. L. Nika, E. P. Pokatilov, A. S. Askerov, A. A. Balandin, *Phys. Rev. B* **2009**, *79*, 155413–155424; d) S. Ghosh, D. L. Nika, E. P. Pokatilov, A. A. Balandin, *New J. Phys.* **2009**, *11*, 095012–095030; e) S. Ghosh, W. Z. Bao, D. L. Nika, S. Subrina, E. P. Pokatilov, C. N. Lau, A. A. Balandin, *Nat. Mater.* **2010**, *9*, 555–558.
- [14] X. Huang, Z. Yin, S. Wu, X. Qi, Q. He, Q. Zhang, Q. Yan, F. Boey, H. Zhang, *Small* **2011**, *7*, 1876–1902.
- [15] H. A. Becerril, J. Mao, Z. Liu, R. M. Stoltenberg, Z. Bao, Y. Chen, *ACS Nano* **2008**, *2*, 463–470.
- [16] A. Das, S. Pisana, B. Chakraborty, S. Piscanec, S. K. Saha, U. V. Waghmare, K. S. Novoselov, H. R. Krishnamurthy, A. K. Geim, A. C. Ferrari, A. K. Sood, *Nat. Nanotechnol.* **2008**, *3*, 210–215.
- [17] Y. Y. Shao, J. Wang, H. Wu, J. Liu, I. A. Aksay, Y. H. Lin, *Electroanal.* **2010**, *22*, 1027–1036.
- [18] L. M. Zhang, J. G. Xia, Q. H. Zhao, L. W. Liu, Z. J. Zhang, *Small* **2010**, *6*, 537–544.
- [19] Z. F. Liu, Q. Liu, Y. Huang, Y. F. Ma, S. G. Yin, X. Y. Zhang, W. Sun, Y. S. Chen, *Adv. Mater.* **2008**, *20*, 3924–3930.
- [20] a) S. M. Paek, E. Yoo, I. Honma, *Nano Lett.* **2009**, *9*, 72–75; b) M. D. Stoller, S. J. Park, Y. W. Zhu, J. H. An, R. S. Ruoff, *Nano Lett.* **2008**, *8*, 3498–3502; c) Y. Wang, Z. Q. Shi, Y. Huang, Y. F. Ma, C. Y. Wang, M. M. Chen, Y. S. Chen, *J. Phys. Chem. C* **2009**, *113*, 13103–13107; d) A. Ghosh, K. S. Subrahmanyam, K. S. Krishna, S. Datta, A. Govindaraj, S. K. Pati, C. N. R. Rao, *J. Phys. Chem. C* **2008**, *112*, 15704–15707.
- [21] a) S. Stankovich, D. A. Dikin, G. H. B. Dommett, K. M. Kohlhaas, E. J. Zimney, E. A. Stach, R. D. Piner, S. T. Nguyen, R. S. Ruoff, *Nature* **2006**, *442*, 282–286; b) J. J. Liang, Y. Huang, L. Zhang, Y. Wang, Y. F. Ma, T. Y. Guo, Y. S. Chen, *Adv. Funct. Mater.* **2009**, *19*, 2297–2302.
- [22] Q. Shao, G. Liu, D. Teweldebrhan, A. A. Balandina, *Appl. Phys. Lett.* **2008**, *92*, 202108–202110.
- [23] C. Berger, Z. M. Song, X. B. Li, X. S. Wu, N. Brown, C. Naud, D. Mayou, T. B. Li, J. Hass, A. N. Marchenkov, E. H. Conrad, P. N. First, W. A. de Heer, *Science* **2006**, *312*, 1191–1196.
- [24] a) A. Reina, X. T. Jia, J. Ho, D. Nezich, H. B. Son, V. Bulovic, M. S. Dresselhaus, J. Kong, *Nano Lett.* **2009**, *9*, 30–35; b) Z. Z. Sun, Z. Yan, J. Yao, E. Beitler, Y. Zhu, J. M. Tour, *Nature* **2010**, *468*, 549–552.
- [25] S. Stankovich, D. A. Dikin, R. D. Piner, K. A. Kohlhaas, A. Kleinhammes, Y. Jia, Y. Wu, S. T. Nguyen, R. S. Ruoff, *Carbon* **2007**, *45*, 1558–1565.
- [26] S. Gilje, S. Han, M. Wang, K. L. Wang, R. B. Kaner, *Nano Lett.* **2007**, *7*, 3394–3398.
- [27] G. Eda, G. Fanchini, M. Chhowalla, *Nat. Nanotechnol.* **2008**, *3*, 270–274.
- [28] S. F. Pei, J. P. Zhao, J. H. Du, W. C. Ren, H. M. Cheng, *Carbon* **2010**, *48*, 4466–4474.

Received: June 30, 2011

Revised: July 20, 2011

Published online: October 11, 2011